



## Comparative molecular field analysis of fenoterol derivatives: A platform towards highly selective and effective $\beta_2$ -adrenergic receptor agonists

Krzysztof Jozwiak<sup>a,\*</sup>, Anthony Yiu-Ho Woo<sup>b</sup>, Mary J. Tanga<sup>c</sup>, Lawrence Toll<sup>c</sup>, Lucita Jimenez<sup>c</sup>, Joseph A. Kozocas<sup>c</sup>, Anita Plazinska<sup>a</sup>, Rui-Ping Xiao<sup>b</sup>, Irving W. Wainer<sup>d</sup>

<sup>a</sup> Department of Chemistry, Medical University of Lublin, Lublin, Poland

<sup>b</sup> Laboratory of Cardiovascular Science, National Institute on Aging Intramural Research Program, Baltimore, MD, United States

<sup>c</sup> SRI International, Menlo Park, CA, United States

<sup>d</sup> Laboratory of Clinical Investigation, National Institute on Aging Intramural Research Program, Baltimore, MD, United States

### ARTICLE INFO

#### Article history:

Received 29 July 2009

Accepted 27 November 2009

Available online 6 December 2009

#### Keywords:

Comparative molecular fields analysis

$\beta_2$  selective agonist

Drug design

### ABSTRACT

**Purpose:** To use a previously developed CoMFA model to design a series of new structures of high selectivity and efficacy towards the  $\beta_2$ -adrenergic receptor. **Results:** Out of 21 computationally designed structures 6 compounds were synthesized and characterized for  $\beta_2$ -AR binding affinities, subtype selectivities and functional activities. **Conclusion:** the best compound is (*R,R*)-4-methoxy-1-naphthylfenoterol with  $K_i\beta_2$ -AR = 0.28  $\mu$ m,  $K_i\beta_1$ -AR/ $K_i\beta_2$ -AR = 573,  $EC_{50cAMP}$  = 3.9 nm,  $EC_{50cardio}$  = 16 nm. The CoMFA model appears to be an effective predictor of the cardiomyocyte contractility of the studied compounds which are targeted for use in congestive heart failure.

© 2009 Elsevier Ltd. All rights reserved.

## 1. Introduction

In the initial studies in this series, (*R,R*)-fenoterol, Fig. 1, a potent and selective  $\beta_2$ -adrenoceptor ( $\beta_2$ -AR) agonist was identified as a potential drug for the treatment of congestive heart failure.<sup>1,2</sup> (*R,R*)-Fenoterol is currently entering initial clinical trials for use in this disease. Based on the potential therapeutic use of (*R,R*)-fenoterol, the stereoisomers of fenoterol and a series of fenoterol analogues were synthesized and tested for  $\beta_2$ -AR activity and selectivity.<sup>3</sup> Three of the 26 compounds investigated in the latter study had submicromolar affinity for the  $\beta_2$ -AR, a >40-fold selectivity for the  $\beta_2$ -AR relative to the  $\beta_1$ -AR and were full agonists of the  $\beta_2$ -AR. One of these compounds, (*R,R*)-methoxyfenoterol was also identified as a potential candidate for drug development and preliminary pharmacokinetic and toxicity studies have been initiated.

The binding affinities,  $K_i$  values, of the 26 fenoterol analogues were used to develop a comparative molecular field analysis model, CoMFA ( $n = 26$ ), to describe and predict the binding of the stereoisomers of fenoterol and fenoterol analogues to the  $\beta_2$ -AR.<sup>3</sup> The CoMFA ( $n = 26$ ) model explained the role of stereoconfiguration and structural modifications of studied molecules on observed  $\beta_2$ -AR affinities. The model was also consistent with earlier findings from other laboratories,<sup>4,5</sup> which indicated that the  $\beta_2$ -AR selectivity of the fenoterol analogues was due to interactions of the aminoalkyl portion of the molecules with different sites within the

transmembrane (TM) components of the  $\beta_2$ -AR. These interactions included hydrogen bond formation between the *p*-oxygen moiety on the phenyl ring in fenoterol and methoxyfenoterol and tyrosine 308 (Y308) in TM7 and/or histidine 296 (H296) in TM6 and  $\pi$ - $\pi$  and/or  $\pi$ -hydrogen bond interactions between the aromatic system of the ligand and aromatic residues located in this area of the binding site. In addition, the data from the previous study<sup>3</sup> and an earlier study<sup>6</sup> indicated that the binding process of the fenoterol analogues with the  $\beta_2$ -AR included the interaction of the chiral center of the aminoalkyl portion with a sterically-restricted site on the receptor.

In this study, the CoMFA ( $n = 26$ ) model was used to design 21 additional fenoterol analogues as potential selective and potent  $\beta_2$ -AR agonists. Based on the CoMFA ( $n = 26$ ) model and the indicated binding interactions, three sites on the aminoalkyl portion of the fenoterol molecule were chosen for alteration, Figure 1. The modifications were utilized to explore the effect on  $\beta_2$ -AR binding affinity, selectivity and agonist activity of the steric bulk

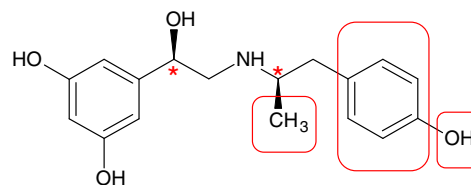


**Figure 1.** The structure of (*R,R*)-fenoterol in which the sites on the molecule probed in this study are circled in red.

\* Corresponding author. Tel.: +48 81 7423686; fax: +48 81 5357350.  
E-mail address: krzysztof.jozwiak@umlub.pl (K. Jozwiak).

at the second chiral center, of a 1-naphthyl versus a 2-naphthyl substituent, and of the effect of a substituent at the 4-position of a 1-naphthyl substituent. A subset of 6 compounds, composed of the (*R,R*)- and (*R,S*)- isomers of 3 of the designed compounds, was synthesized using the previously described approach.<sup>3</sup> The  $\beta_2$ -AR and  $\beta_1$ -AR binding affinities and the  $EC_{50}$  values associated with induced cAMP accumulation ( $EC_{50cAMP}$ ) were determined. The (*R,R*)-isomers of the subset were tested for their activity in a previously described cardiomyocyte contractility model<sup>3</sup> and their  $EC_{50cardio}$  values determined.

## 2. Results

In the previous study, the CoMFA( $n = 26$ ) model was derived using the experimentally determined  $\beta_2$ -AR binding affinities of a training set of 26 fenoterol derivatives and stereoisomers.<sup>3</sup> The validity parameters of the model were high ( $R^2 = 0.920$ ,  $Q^2 = 0.847$ ,  $F = 60.380$ ) and the standard error of prediction was low (SEP = 0.309). In the current study, the CoMFA( $n = 26$ ) model was used to estimate the  $pK_i$  values for the (*R,R*)-isomers of a set of 12 new molecular structures, and the (*R,S*)-, (*S,R*)- and (*S,S*)-isomers of three of these compounds for a set of 21 unique compounds, **52–63**, Table 1.

The (*R,R*)- and (*R,S*)-isomers of three of the designed fenoterol analogues, **52**, **53**, **54**, were synthesized using a previously described synthetic scheme in which the epoxide formed from (*R*)-(-)-3',5'-dibenzoyloxyphenylbromohydrin was coupled with the (*R*)- or (*S*)-enantiomer of the appropriate *N*-benzylamino-alkanes.<sup>3</sup> The chirality of the first asymmetric center was set as (*R*) based on the data from the previous study that fenoterol analogues with this configuration had higher affinities and activities at the  $\beta_2$ -AR relative to the corresponding analogues with a (*S*)-configuration at this carbon.<sup>3</sup>

The binding affinities of the synthesized compounds were determined using membranes derived from HEK cells stably transfected with human  $\beta_2$ -AR and  $\beta_1$ -AR as previously described<sup>3</sup> and the corresponding  $K_i$  values were calculated, Table 2. The maximum difference,  $\Delta$  value, between computationally predicted and experimentally determined affinities, expressed as  $pK_i$  values ( $-\log K_i$ ), was  $-0.6$  and in some cases did not exceed the standard error of experimental determination, Table 1. The external validation of the CoMFA( $n = 26$ ) model with the newly synthesized test set was calculated and the results,  $R^2_{PRED} = 0.583$ ,  $S_{PRESS} = 0.337$ , where PRESS is predictive residual sum of squares,  $\sum(\Delta^2)^7$ , indicated that the CoMFA( $n = 26$ ) model had a high predictive power for the computational design of congeneric  $\beta_2$ -AR agonists based upon fenoterol.

The  $\beta_2$ -AR and  $\beta_1$ -AR binding affinities,  $K_i(\beta_2\text{-AR})$  and  $K_i(\beta_1\text{-AR})$ , and relative binding affinities,  $K_i(\beta_1\text{-AR})/K_i(\beta_2\text{-AR})$ , of the (*R,R*)- and (*R,S*)- isomers of **52**, **53** and **54**, were determined, Table 2. In addition, the  $\beta_2$ -AR agonist activities of the (*R,R*)-isomers of the previously reported compounds **1**, **2**, **5** and **52**, **53**, **54** were examined using a previously described cardiomyocyte contractility model, Table 3.<sup>3</sup> In these studies, the agonist-stimulated  $\beta_2$ -AR contractility response was distinguished from that of  $\beta_1$ -AR activity using ICI 118,551, a  $\beta_2$ -AR specific antagonist.

The data demonstrate that the substitution of the methyl group by an ethyl moiety at the chiral center on the aminoalkyl portion of the fenoterol backbone, **1** and **52**, respectively, reduced the calculated binding affinities to the  $\beta_2$ -AR. The  $K_i(\beta_2\text{-AR})$  value for (*R,R*)-**52** was  $\sim 4$ -fold greater than that of (*R,R*)-**1** and the value for (*R,S*)-**52** was 1.5-fold greater than that of (*R,S*)-**1**, Table 2. The binding affinities to the  $\beta_1$ -AR were also affected, as the  $K_i(\beta_1\text{-AR})$  of (*R,R*)-**52** was 28-fold higher than that of (*R,R*)-**1** and the  $K_i(\beta_1\text{-AR})$  for (*R,S*)-**52** was sixfold greater than that of (*R,S*)-**1**. The greater

reductions in the affinity to the  $\beta_1$ -AR were reflected in the relative binding affinities as the  $K_i(\beta_1\text{-AR})/K_i(\beta_2\text{-AR})$  for the (*R,R*)-isomers increased from 43 (**1**) to 334 (**52**) and from 5 (**1**) to 20 (**52**) for the (*R,S*)-isomers. Thus, a modest increase in the steric bulk at the chiral center on the aminoalkyl portion of the molecule increased the relative energies of the agonist- $\beta_2$ -AR and agonist- $\beta_1$ -AR complexes, irrespective of the configuration at that site. These results are consistent with the existence of a sterically-restricted site on the  $\beta_2$ -AR and suggest that the site is also present in the  $\beta_1$ -AR and that the steric interaction has a stronger effect on the binding to the  $\beta_1$ -AR.

The substitution of an ethyl moiety for the methyl group produced a slight but significant increase in the  $EC_{50cAMP}$  values of (*R,R*)- and (*R,S*)-**52** relative to (*R,R*)- and (*R,S*)-**1**, Table 3. However, the increase in steric bulk produced a profound decrease in the activity of (*R,R*)-**52** in the cardiomyocyte contractility model as the  $EC_{50cardio}$  of (*R,R*)-**52** was 8551 nM, a 128-fold increase relative to (*R,R*)-**1**,  $EC_{50cardio} = 83$  nM, Table 3. Thus it appears that steric interactions involving the chiral center on the aminoalkyl portion of the fenoterol molecule had a greater effect in  $\beta_2$ -AR associated cardiomyocyte contractility system than in the displacement binding or cAMP stimulation studies. It is interesting to note that the activity of (*R,R*)-**52** in the cardiomyocyte contractility model was antagonized by the  $\beta_2$ -AR selective antagonist ICI 118,551, but (*R,R*)-**52** did not antagonize the activity of zinterol in this model (data not shown).

When the effect of the change in the orientation of a naphthyl moiety on the aminoalkyl portion of the molecule from the 1- to the 2-position on the ring, **5** and **53**, was investigated, the data indicate that this change had only a slight effect on the binding affinities to the  $\beta_2$ -AR and  $\beta_1$ -AR, Table 2. In these studies, the differences between the  $K_i(\beta_2\text{-AR})$  for the (*R,R*)- and (*R,S*)- isomers of **53** and the corresponding isomers of **5** were less than twofold as was the difference in the  $K_i(\beta_1\text{-AR})$  for (*R,S*)-**53** and (*R,S*)-**5**. The greatest effect was seen in the  $K_i(\beta_1\text{-AR})$  of (*R,R*)-**53** which was  $\sim 4$ -fold higher relative to that of (*R,R*)-**5**, and reflected in an increase in the relative binding affinities,  $K_i(\beta_1\text{-AR})/K_i(\beta_2\text{-AR})$  from 14 (**5**) to 40 (**53**). The results suggest that the change from a 1-naphthyl to a 2-naphthyl substituent on the fenoterol molecule had a relatively small effect on the  $\pi$ - $\pi$  and/or  $\pi$ -hydrogen bond interactions between the naphthyl substituent and aromatic residues located in this area of the binding site of the  $\beta_2$ -AR. The data also suggest that these interactions occur between the agonists and the  $\beta_1$ -AR.

While the change from a 1-naphthyl to a 2-naphthyl substituent has less than a twofold affect on the  $K_i(\beta_2\text{-AR})$  of the (*R,R*)-isomers, a greater effect was seen in the  $EC_{50cAMP}$  values as the  $EC_{50cAMP}$  of (*R,R*)-**53** was 30-fold lower than that of (*R,R*)-**5**, Table 3. However, the inverse was observed with cardiomyocyte contractility as the  $EC_{50cardio}$  of (*R,R*)-**53** was threefold higher than that of (*R,R*)-**5**, Table 3, but it is not clear if this difference has any pharmacological significance. There was less than a threefold difference in the  $EC_{50cAMP}$  values (*R,S*)-**53** and (*R,S*)-**5**, Table 3.

The data from the initial studies of the aminoalkyl analogues of fenoterol, indicated that optimum binding affinities and  $\beta_2$ -AR selectivities were observed with an electronegative substituent in the 4-position of the benzyl moiety or with a 1-naphthyl moiety.<sup>3</sup> In this study, a series of 4-substituted-1-naphthyl analogues of fenoterol, **54–63**, were docked in the CoMFA( $n = 26$ ) model and their  $pK_i$  values predicted, Table 1. The results indicated that the presence of an electronegative substituent increased the binding affinity of the compound and that the  $pK_i$  values of the (*R,R*)-isomers of **54–59** would be greater than the corresponding values of **1**, **2** and **5**. It is of interest to note that 4-amino-1-naphthylfenoterol (**60**) had the lowest predicted  $pK_i$  which is consistent with the previous

**Table 1**  
Computationally predicted  $pK_i$  values [ $pK_i(\text{CoMFA})$ ] for the compounds designed using the previously reported CoMFA( $n = 26$ ) model<sup>3</sup>

No.	Structure	Stereochemistry/substitution	$pK_i$ CoMFA	$pK_i$ exper.	$\Delta$
<i>Old compounds</i>					
1		( <i>R,R</i> )	5.84	6.46	-0.62
		( <i>R,S</i> )	5.48	5.43	0.05
		( <i>S,R</i> )	5.02	4.99	0.03
		( <i>S,S</i> )	4.66	4.56	0.10
2		( <i>R,R</i> )	6.17	6.32	-0.15
		( <i>R,S</i> )	5.80	5.71	0.09
		( <i>S,R</i> )	5.34	5.28	0.06
		( <i>S,S</i> )	4.99	4.80	0.19
3		( <i>R,R</i> )	5.57	5.53	0.04
		( <i>R,S</i> )	5.21	5.10	0.11
		( <i>S,R</i> )	4.75	4.64	0.11
		( <i>S,S</i> )	4.39	4.54	-0.15
5		( <i>R,R</i> )	6.72	6.62	0.10
		( <i>R,S</i> )	6.36	6.47	-0.11
		( <i>S,R</i> )	5.90	5.75	0.15
		( <i>S,S</i> )	5.54	5.60	-0.06
<i>New compounds</i>					
52		( <i>R,R</i> )	5.91	5.895	0.015
		( <i>R,S</i> )	5.47	5.240	0.23
		( <i>S,R</i> )	5.08		
		( <i>S,S</i> )	4.65		
53		( <i>R,R</i> )	6.04	6.393	-0.353
		( <i>R,S</i> )	5.7	6.293	-0.593
		( <i>S,R</i> )	5.2		
		( <i>S,S</i> )	5.2		
54		( <i>R,R</i> )	6.93	6.556	0.374
		( <i>R,S</i> )	6.6	6.498	0.102
		( <i>S,R</i> )	6.24		
		( <i>S,S</i> )	5.91		
55		R = OH	6.79		
56		R = F	6.76		
57		R = Cl	6.92		
58		R = Br	6.94		
59		R = CF <sub>3</sub>	6.95		
60		R = NH <sub>2</sub>	5.79		
61		R = CH <sub>3</sub>	6.41		
62		R = SH	6.38		
63		R = SCH <sub>3</sub>	6.40		
<u>(<i>R,R</i>) isomers only</u>					

study in which the  $K_i(\beta_2\text{-AR})$  of (*R,R*)-4-aminobenzylfenoterol (**4**) was greater than the corresponding values for **1**, **2** and **5**.<sup>3</sup>

In this study, (*R,R*)-**54** and (*R,S*)-**54** were synthesized and tested. The data obtained with (*R,R*)-**54** indicate that the  $\beta_2\text{-AR}$  binding

**Table 2**

Experimentally determined binding affinities to the  $\beta_2$ -adrenergic receptor ( $K_i$   $\beta_2$ -AR) and  $\beta_1$ -adrenergic receptor ( $K_i$   $\beta_1$ -AR) of the compounds synthesized in this study and previously reported compounds, the relative  $\beta_1$ -AR and  $\beta_2$ -AR binding affinities ( $K_i$   $\beta_1$ / $K_i$   $\beta_2$ )

	$K_i$ $\beta_1$ -AR ( $\mu$ M)	$K_i$ $\beta_2$ -AR ( $\mu$ M)	$K_i$ $\beta_1$ / $K_i$ $\beta_2$
( <i>R,R</i> )- <b>1</b>	14.8 $\pm$ 2.5 <sup>a</sup>	0.35 $\pm$ 0.03 <sup>a</sup>	43 <sup>a</sup>
( <i>R,S</i> )- <b>1</b>	18.9 $\pm$ 2.4 <sup>a</sup>	3.69 $\pm$ 0.25 <sup>a</sup>	5 <sup>a</sup>
( <i>R,R</i> )- <b>2</b>	21.9 $\pm$ 3.1 <sup>a</sup>	0.47 $\pm$ 0.04 <sup>a</sup>	47 <sup>a</sup>
( <i>R,S</i> )- <b>2</b>	30.8 $\pm$ 2.5 <sup>a</sup>	1.93 $\pm$ 0.14 <sup>a</sup>	16 <sup>a</sup>
( <i>R,R</i> )- <b>5</b>	3.35 $\pm$ 0.13 <sup>a</sup>	0.24 $\pm$ 0.03 <sup>a</sup>	14 <sup>a</sup>
( <i>R,S</i> )- <b>5</b>	15.8 $\pm$ 2.5 <sup>a</sup>	0.34 $\pm$ 0.03 <sup>a</sup>	46 <sup>a</sup>
( <i>R,R</i> )- <b>52</b>	424.3 $\pm$ 70.7	1.27 $\pm$ 0.81	334
( <i>R,S</i> )- <b>52</b>	116.7 $\pm$ 44.4	5.76 $\pm$ 0.83	20
( <i>R,R</i> )- <b>53</b>	16.6 $\pm$ 1.6	0.41 $\pm$ 0.09	40
( <i>R,S</i> )- <b>53</b>	27.1 $\pm$ 2.6	0.51 $\pm$ 0.06	53
( <i>R,R</i> )- <b>54</b>	160.5 $\pm$ 54.1	0.28 $\pm$ 0.01	573
( <i>R,S</i> )- <b>54</b>	14.8 $\pm$ 1.6	0.32 $\pm$ 0.01	46

<sup>a</sup>  $K_i$   $\beta_2$ -AR and  $K_i$   $\beta_1$ -AR values obtained from Ref. 3.

**Table 3**

The activity (presented as  $EC_{50}$  values) of the (*R,R*)- and (*R,S*)-isomers of fenoterol and selected fenoterol analogues in the stimulation of cAMP accumulation in HEK cells containing human  $\beta_2$ -adrenergic receptors ( $EC_{50cAMP}$ ) and in a cardiomyocyte contractility model system ( $EC_{50cardio}$ )

	Induced stimulation of cAMP accumulation		Cardiomyocyte contractility
	$EC_{50cAMP}$ (nM)	% Stimulation	$EC_{50cardio}$ (nM)
( <i>R,R</i> )- <b>1</b>	0.30 $\pm$ 0.09	123 $\pm$ 9	73 $\pm$ 18
( <i>R,S</i> )- <b>1</b>	4.70 $\pm$ 0.50	131 $\pm$ 30	575 $\pm$ 122
( <i>R,R</i> )- <b>2</b>	0.30 $\pm$ 0.23	136 $\pm$ 11	186 $\pm$ 50
( <i>R,S</i> )- <b>2</b>	2.00 $\pm$ 0.45	120 $\pm$ 19	506 $\pm$ 107
( <i>R,R</i> )- <b>5</b>	12.50 $\pm$ 3.50	129 $\pm$ 24	59 $\pm$ 16
( <i>R,S</i> )- <b>5</b>	2.70 $\pm$ 0.84	112 $\pm$ 42	103 $\pm$ 34
( <i>R,R</i> )- <b>52</b>	2.80 $\pm$ 0.90	125 $\pm$ 6	8551 $\pm$ 4992
( <i>R,S</i> )- <b>52</b>	16.60 $\pm$ 4.90	98 $\pm$ 4	
( <i>R,R</i> )- <b>53</b>	0.40 $\pm$ 0.12	90 $\pm$ 10	133 $\pm$ 25
( <i>R,S</i> )- <b>53</b>	7.60 $\pm$ 2.76	89 $\pm$ 12	
( <i>R,R</i> )- <b>54</b>	3.90 $\pm$ 1.80	106 $\pm$ 11	16 $\pm$ 4
( <i>R,S</i> )- <b>54</b>	4.00 $\pm$ 1.29	118 $\pm$ 30	

affinity of this compound was equivalent to (*R,R*)-**5** and slightly stronger than (*R,R*)-**2**, Table 2. The same trend was observed with the (*R,S*)-isomers as the  $K_i$ ( $\beta_2$ -AR) values of (*R,S*)-**54** and (*R,S*)-**5** were equivalent and both were about sixfold stronger than (*R,S*)-**2**. The results suggest that when both a *p*-methoxy moiety and a 1-naphthyl moieties are present in the molecule, interactions with the naphthyl group appear to play a more significant role in the stabilization of the agonist- $\beta_2$ -AR complex.

The  $K_i$ ( $\beta_1$ -AR) value of (*R,R*)-**54** was significantly weaker than (*R,R*)-**2** (19-fold) and (*R,R*)-**5** (141-fold), while there was no significant difference between (*R,S*)-**54** and the (*R,S*)-isomers of **2** and **5**, Table 2. The weaker  $\beta_1$ -AR binding affinity for (*R,R*)-**54** was reflected in the relative binding affinity ratios,  $K_i$ ( $\beta_1$ -AR)/ $K_i$ ( $\beta_2$ -AR) which increased to 573, as compared to 47 and 14, for (*R,R*)-**2** and (*R,R*)-**5**, respectively. The results indicate that both the *p*-methoxy and 1-naphthyl moieties in (*R,R*)-**54** had a destabilizing effect in the binding interactions with the  $\beta_1$ -AR relative to the (*R,R*)-isomers of **2** and **5**. This effect was not observed in the relative binding of the (*R,S*)-isomers of **54**, **2** and **5** to the  $\beta_1$ -AR suggesting that the *S*-configuration in the aminoalkyl portion of the molecule altered the role of the 4-oxy and/or 1-naphthyl substituents in the binding of (*R,S*)-**54** to the  $\beta_1$ -AR.

While the  $K_i$ ( $\beta_2$ -AR) values of the (*R,R*)-isomers of **2**, **5** and **54** were essentially equivalent, the  $EC_{50cAMP}$  values of **5** and **54** were significantly higher, 40-fold and 10-fold, respectively, than the  $EC_{50cAMP}$  value of **2**, Table 3. If the  $EC_{50cAMP}$  value of (*R,R*)-**1** is also

considered, then the data suggest that fenoterol analogues containing a *p*-oxy-phenyl moiety have a greater effect on cAMP stimulation than fenoterol analogues containing a 1-naphthyl moiety, **5**, and that the addition of a 4-methoxy substituent in the naphthyl ring has a positive effect on the  $EC_{50cAMP}$  value, **54**. It is of interest to note that there is no significant difference in the  $EC_{50cAMP}$  values of (*R,R*)-**2** and (*R,R*)-**53**, which contains a 2-naphthyl ring. This suggests that the difference in the  $EC_{50cAMP}$  values between **2** and **5** is a function of the relative position of the naphthyl group within the  $\beta_2$ -AR binding area rather than the lack of a *p*-oxy-substituent.

When the effect on cardiomyocyte contractility was investigated, the relative  $EC_{50cardio}$  values were **54** < **5** < **2**, although the difference between **54** and **2** was only  $\sim$ 10-fold. These results indicate that the presence of the 1-naphthyl ring and the 4-methoxy substituent had a synergistic effect in this model system.

No significant differences were observed in the cAMP stimulation produced by the (*R,S*)-isomers of **2**, **5**, and **54**, Table 3. For these compounds, the relative differences between the (*R,R*)- and (*R,S*)-isomers of each compound mirrored the relative differences in  $K_i$ ( $\beta_2$ -AR) values, that is, (*R,R*)-**2** < (*R,S*)-**2**; (*R,R*)-**5** > (*R,S*)-**5**; (*R,R*)-**54**  $\approx$  (*R,S*)-**54**, Tables 2 and 3. These results suggest that the displacement binding studies and the induced stimulation of cAMP accumulation may reflect the same binding process.

The  $pK_i$  data from this study was used to refine the CoMFA ( $n = 26$ ) model. A total of 32 structures (26 original and 6 newly synthesized) were used as the training set for a revised 3D-QSAR model, CoMFA ( $n = 32$ ). Partial Least Square methodology extracted four statistically significant components of the model, and all of the validation parameters were high and indicated that the model had a stronger predictive power than the CoMFA ( $n = 26$ ) model, Table 4.

**Table 4**

Quantitative comparison of the refined CoMFA ( $n = 32$ ) model with the original model, CoMFA ( $n = 26$ )<sup>3</sup>

	CoMFA ( $n = 26$ )	CoMFA ( $n = 32$ )
$n$	26	32
PLS components	4	4
$R^2$	0.920	0.925
$F(n_1, n_2)$	60.380 (4, 21)	64.984 (4, 27)
$Q^2(100)$	0.847	0.851
SEE	0.223	0.216
SEP	0.309	0.305
Electrostatic contribution	48.1%	38.3%
Steric contribution	51.9%	61.7%

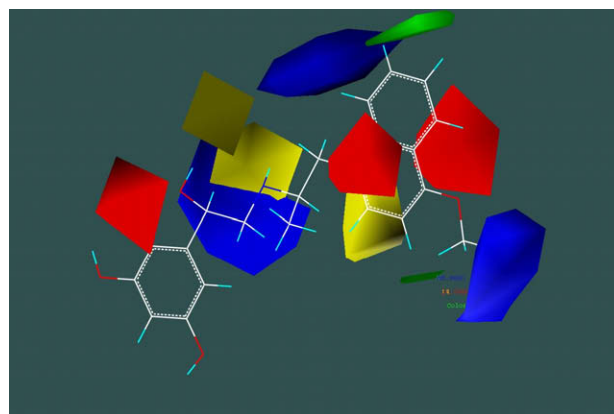


**Figure 2.** The CoMFA ( $n = 32$ ) model with (*R,R*)-**54** included in the figure. The fields are color coded in the following manner: green represents a region of favorable steric (bulk) interactions, unfavorable steric interactions are denoted by yellow, electrostatic interactions with a positive charge (or H-bond donors) are blue, and electrostatic interactions with a negative charge (or H-bond acceptors) are red.

The CoMFA( $n = 32$ ) model is presented in Fig. 2. For visual clarity only (*R,R*)-**54** is included in the figure. The interaction fields are color coded in the following manner: green represents a region of favorable steric (bulk) interactions, unfavorable steric interactions are denoted by yellow, electrostatic interactions with a positive charge (or H-bond donors) are blue, and electrostatic interactions with a negative charge (or H-bond acceptors) are red.

As previously demonstrated with the CoMFA( $n=26$ ) model, the CoMFA( $n = 32$ ) model explains the source of stereoselectivity observed with this group of compounds. At the first center of chirality, an *R*-configuration directs the hydroxyl moiety towards the negative charge field (red), a favorable interaction, while an *S*-configuration at this center directs the hydroxyl moiety towards the positive charge field, a destabilizing interaction. Steric fields are associated with both chiral centers and an *S*-configuration at both of the sites directs substituents toward an unfavorable steric interaction site, denoted by the yellow fields.

The interactions of the aminoaryl portion of the fenoterol analogues with the  $\beta_2$ -AR and the relative stabilities of the agonist-receptor complexes were also refined in the CoMFA( $n = 32$ ) model. These interactions are illustrated by the proposed stabilizing interactions associated with the 4-methoxy-1-naphthyl substituent of (*R,R*)-**54**, Fig. 2. In this model, the substituent is placed in the vicinity of electrostatic interactions with a positive charge or H-bond donors (blue regions), suggesting hydrogen bond interaction with the oxygen atom. Additional stabilizing interactions are suggested by the presence of two large electronegative fields (red regions) surrounding both faces of the naphthyl ring of the (*R,R*)-**54** indicating the possibility of  $\pi$ - $\pi$  interactions with aromatic residues within the binding site. Steric favoring regions (green regions) are also present at both edges of the naphthyl ring, which most probably reflects the preference of 1-naphthyl versus 2-naphthyl in the  $\beta_2$ -AR binding. These regions may also affect the conformational mobility of a molecule during the optimization of electrostatic and  $\pi$ - $\pi$  interactions. The three interaction sites are independent and appear to act cooperatively in the binding of (*R,R*)-**54**.

### 3. Discussion

The results of this study demonstrate that the CoMFA( $n = 26$ ) model can be used to design selective  $\beta_2$ -AR agonists based upon fenoterol or compounds that contain interactive sites equivalent to those found on the aminoalkyl portion of the fenoterol molecule. This design strategy is reflected by the synthesis and properties of the  $\beta_2$ -AR agonist (*R,R*)-**54**, which is highly selective ( $K_i(\beta_1)/K_i(\beta_2) = 573$ ) and effective ( $EC_{50} = 16$  nM, cardiomyocyte contractility).

The revised molecular model, CoMFA( $n = 32$ ) is consistent with the earlier model<sup>3</sup> and with the previously reported models describing the molecular basis of  $\beta_2$ -AR selectivity,<sup>4–6</sup> although a recent paper has questioned the role that Y308 plays in this process.<sup>8</sup> The data from this study supports the hypothesis that hydrogen bond formation between the *p*-oxygen moiety on the aromatic substituents of the (*R,R*)-isomers of **1**, **2**, **52**, and **54** and Y308 in TM7 and/or H296 in TM6 contribute to the >40-fold  $\beta_2$ -AR selectivity. The role of Y308 in  $\beta_2$ -AR selective binding was also supported by the data from a study of the binding of salmeterol to chimeric  $\beta_1/\beta_2$ -ARs and alanine-substituted  $\beta_2$ -AR mutants.<sup>5</sup> In these studies, the  $K_i(\beta_2)$  changed from 1.5 nM in the wild-type receptor to 184 nM in the Y308A mutant, the largest effect observed in the series of alanine-substituted  $\beta_2$ -AR mutants used in the study.

The data also indicate that the >300-fold  $\beta_1$ -AR/ $\beta_2$ -AR selectivity of (*R,R*)-**52** and (*R,R*)-**54** was primarily due to a large decrease in  $\beta_1$ -AR binding affinities, Table 2. It is reasonable to assume that the weaker affinities reflect the loss of hydrogen bond interactions due to the replacement of Y308 and H296 in the  $\beta_2$ -AR by F359 and K347, respectively, in the  $\beta_1$ -AR.<sup>6</sup> This hypothesis is supported by

binding studies with the wild-type  $\beta_1$ -AR and  $\beta_2$ -AR and salmeterol and a salmeterol derivative that lacked an ether linkage found in the parent compound.<sup>5</sup> The  $K_i(\beta_2)$ -AR) of salmeterol and the derivative were 1.5 nM and 220 nM, respectively, while the  $K_i(\beta_1)$ -AR) values were both  $\sim 2300$  nM. The differences in the  $K_i(\beta_2)$ -AR) values were reflected in the  $K_i(\beta_1)$ -AR)/ $K_i(\beta_2)$ -AR) ratios which were >1000 for salmeterol and  $\sim 10$  for the derivative. The authors of this study concluded that the large difference in the relative binding ratios was a result of the inability of the derivative to interact with Y308 in the  $\beta_2$ -AR due to the absence of the oxygen atom of the ether linkage.

The >500-fold  $\beta_2$ -AR selectivity observed with (*R,R*)-**54** and the >40-fold  $\beta_2$ -AR selectivity observed with compounds that do not contain *p*-oxygen moieties, that is, (*R,S*)-**5**, (*R,R*)-**53**, (*R,S*)-**53**, Table 2, indicate that  $\pi$ - $\pi$  and/or  $\pi$ -hydrogen bond interactions also play a role in the relative stabilities of the two  $\beta$ -ARs. The contribution of  $\pi$ - $\pi$  and/or  $\pi$ -hydrogen bond interactions in the binding process is indicated by the two electronegative fields in the CoMFA( $n = 32$ ) model, which are located on both faces of the docked (*R,R*)-**54**, Fig. 2. The electronegative fields in the CoMFA( $n = 32$ ) model reflect a network of  $\pi$ - $\pi$  interactions which include Y308 in the  $\beta_2$ -AR and other aromatic residues such as H296, Y316, F289, F193, F290 and W109 which are in close proximity to Y308.<sup>9</sup> The higher  $K_i(\beta_1)$ -AR) values for the same compounds suggest that  $\pi$ - $\pi$  interaction networks based upon F325 and other aromatic residues also exist in the  $\beta_1$ -AR, but that the interactions are weaker than the corresponding ones in the  $\beta_2$ -AR. In addition, the presence of extended electronegative fields in both  $\beta$ -ARs also explains the lack of a significant difference in the affinities of the 1-naphthyl and 2-naphthyl analogues, except for the interaction of (*R,R*)-**54** with the  $\beta_1$ -AR. In this case, the 4-methoxy substituent may play a more significant role in the increased  $K_i(\beta_1)$ -AR) value than the 1-naphthyl ring.

In the initial study involving the stereoisomers of fenoterol and fenoterol analogues<sup>3</sup> and with the compounds synthesized in this study, the  $\beta_2$ -AR binding affinities of the (*R,R*)-isomers were greater than the corresponding (*R,S*)-isomers. The results support the hypothesis that the stereochemistry of the chiral carbon on the aminoalkyl moiety positions this portion of the molecule relative to the interactive moieties in TM3, TM6 and TM7 and that this effect reflects interactions with a sterically-restricted site on the  $\beta_2$ -AR.<sup>3</sup> These data indicate that this effect was more pronounced with compounds containing a phenyl ring with a *p*-hydroxy or *p*-methoxy substituent, that is, **1**, **2**, **52**, Table 2. This may reflect the fact that the hydrogen bonding interactions between the *p*-substituents on **1**, **2** and **52** and the  $\beta_2$ -AR occur at more defined sites, that is, Y308 and H296, than the sites binding to non-oxygen containing fenoterol analogues, that is, a diffuse  $\pi$ - $\pi$  interaction area. Therefore, subtle changes in the binding interactions produced by alterations in the relative positions of the (*R,R*)- and (*R,S*)-isomers should have a greater effect in **1**, **2**, and **52** than **5** and **53**. The minimal differences between the  $K_i(\beta_2)$ -AR) values of (*R,R*)-**54** and (*R,S*)-**54** suggests that the  $\pi$ - $\pi$  interactions play a relatively larger role in the stabilization of the **54**- $\beta_2$ -AR complex than the hydrogen bonding interactions.

In this study, the  $K_i(\beta_1)$ -AR) values of the (*R,R*)-isomers of **1**, **2**, **5**, and **53** were lower than the corresponding (*R,S*)-isomers although the calculated differences were <5-fold, Table 2. The opposite effect was observed with **52** and **54** where the  $K_i(\beta_1)$ -AR) of the (*R,R*)-isomers were 4-fold and 10-fold larger, respectively, Table 2. The  $K_i(\beta_1)$ -AR)/ $K_i(\beta_2)$ -AR) ratios of **52** and **54** were also significantly greater than those observed with the other fenoterol analogues, by 334- and 573-fold, respectively. The results obtained with **52** may reflect the effect of the increase in steric bulk at the chiral center and the resulting destabilization of the **52**- $\beta_1$ -AR complexes, irrespective of the chirality, as both isomers have  $K_i(\beta_1)$ -AR) values

>100  $\mu\text{M}$ . This suggests that the postulated sterically-restricted site on the  $\beta_2$ -AR also exist in the  $\beta_1$ -AR.

When the results obtained with **54** are compared to **2** and **5**, it is evident that for (*R,S*)-**54**, the presence of both a 4-methoxy moiety and a 1-naphthyl moiety had little effect on the  $K_i(\beta_1\text{-AR})$  relative to the presence of only a 4-methoxy moiety or a 1-naphthyl moiety, (*R,S*)-**2** and (*R,S*)-**5**, respectively, Table 2. The more significant effect is seen with (*R,R*)-**54** as the calculated  $K_i(\beta_1\text{-AR})$  increased from 21.9  $\mu\text{M}$  (**2**) and 3.35  $\mu\text{M}$  (**5**) to 160.5  $\mu\text{M}$ . The results indicate that the presence of the 4-methoxy and 1-naphthyl moieties act in a synergistic manner to reduce the stability of the (*R,R*)-**54**- $\beta_1$ -AR complex. The mechanism associated with this phenomenon is currently unknown.

The 12 compounds used in this study stimulated cAMP accumulation with  $EC_{50(\text{cAMP})}$  values that ranged from 0.30 nM to 16.60 nM, Table 3, and all of these compounds can be classified as full  $\beta_2$ -AR agonists. There was no direct relationship between the  $K_i(\beta_2\text{-AR})$  and  $EC_{50(\text{cAMP})}$  values probably due to the fact that the binding studies used a radiolabeled antagonist. Planned studies with a radiolabeled fenoterol analog may produce a better correlation between binding affinity and stimulation of cAMP accumulation. The fact that fenoterol analogs stimulate cAMP affinity at considerably lower concentrations than they stimulate cardiomyocyte contractility suggests either a far greater degree of amplification in the cAMP activity pathway, or potentially a different signal transduction pathway altogether.

In the cardiomyocyte contractility model system, 8 of the 9 compounds studied had stimulatory effects with  $EC_{50(\text{cardio})}$  values ranging from 16 ((*R,R*)-**54**) to 575 nM ((*R,S*)-**1**), Table 3. The clear outlier was (*R,R*)-**52** with an  $EC_{50(\text{cardio})}$  value of 8551 nM. When the  $K_i(\beta_2\text{-AR})$  and  $EC_{50(\text{cardio})}$  values for the 8 compounds were compared, there was a statistically significant relationship between the values,  $r^2 = 0.8804$ ,  $p = 0.006$ . The data indicate that in a series of fenoterol analogues a  $K_i(\beta_2\text{-AR})$  of  $\leq 0.500 \mu\text{M}$  should correspond to a  $EC_{50(\text{cardio})}$  of  $< 0.200 \mu\text{M}$  and that the CoMFA models described in these studies are capable of designing compounds which are active agonists in the  $\beta_2$ -AR cardiomyocyte contractility model. The  $EC_{50(\text{cardio})}$  value obtained with (*R,R*)-**52** was similar to previous data obtained with (*S,R*)-**1** and (*S,R*)-**2**,  $EC_{50(\text{cardio})} = 2340 \text{ nM}$  and  $3160 \text{ nM}$ , respectively.<sup>10</sup> It is of interest to note that all three compounds can be classified as full  $\beta_2$ -AR agonists with respect to cAMP stimulation,  $EC_{50(\text{cAMP})} = 2.80$  ((*R,R*)-**52**),  $8.50 \text{ nM}$  ((*S,R*)-**1**),  $7.20 \text{ nM}$  ((*S,R*)-**2**). The data indicate that the chirality at both of the chiral centers on the fenoterol backbone and the steric bulk at the second chiral center play limited roles in cAMP stimulation, but a major role in cardiomyocyte contractility. The role of the chiral centers in cardiomyocyte contractility has been previously demonstrated in which (*R,R*)-**1** and (*R,R*)-**2** were shown to preferentially activate  $G_s$  signaling while the corresponding (*S,R*)-isomers activated both  $G_s$  and  $G_i$  proteins.<sup>10</sup> Our initial data indicate that the cardiomyocyte contractility of (*R,R*)-**52** is consistent with the selectivity of the (*S,R*)-isomers as this activity is sensitive to pertussis toxin, which indicates that this compound activates both  $G_s$  and  $G_i$  proteins (data not shown).

The data from this study are consistent with the hypothesis that there are two binding areas within the  $\beta_2$ -AR molecule. One area is the site that interacts with the 'catechol' portion of an agonist and is created by residues in TM3, TM5 and TM6, (the 'first' binding area).<sup>7,11–15</sup> The "second" binding area is created by residues in TM3, TM6 and TM7 and interacts with the aminoalkyl side chain of the fenoterol analogues.<sup>3–6</sup> The results also suggest that the binding process between the fenoterol analogues and the  $\beta_2$ -AR involves a number of multi-step interactions. In addition, these interactions and their functional consequences vary based upon the composition and stereochemistry of the fenoterol analogue.

The binding of an agonist to the  $\beta_2$ -AR has been previously described as a multi-step sequential process that produces a series of conformational changes in the receptor.<sup>14,15</sup> This description reflects the extensive study of the binding of agonists to the 'first' binding area and it is important to note that the majority of the compounds used in these studies did not have large amino alkyl side chains containing oxygen or aromatic moieties, cf. Ref. 13. Thus it is reasonable to assume that with compounds such as the fenoterol analogues, the sequential binding mechanism will also include interactions with the 'second' binding area and that these interactions will also result in distinct conformational changes in the  $\beta_2$ -AR molecule. However, the data from the current study are unable to differentiate between these binding interactions. This is in part due to the fact that the binding studies were conducted using [<sup>3</sup>H]CGP-12177, a highly selective  $\beta_2$ -AR antagonist, which, unfortunately, does not contain a fenoterol-like alkylamino moiety.<sup>16</sup> This issue is being addressed in binding studies using a [<sup>3</sup>H]-labeled fenoterol analogue as the marker ligand and in molecular modeling and thermodynamic studies, which have also been initiated.

## 4. Experimental section

### 4.1. $\beta_2$ -AR binding assays

Compounds synthesized in this study were tested up to three times each to determine their binding affinities at the  $\beta_1$ - and  $\beta_2$ -ARs following a previously described approach.<sup>3</sup> In brief,  $\beta_2$ -AR binding was conducted on membranes derived from HEK cells containing human  $\beta_2$ -AR (provided by Dr. Brian Kobilka, Stanford Medical Center, Palo Alto, CA). Cells were grown in Dulbecco's Modified Eagle Medium (DMEM) containing 10% fetal bovine serum (FBS) and 0.05% penicillin–streptomycin with 400  $\mu\text{g}/\text{mL}$  G418.  $\beta_1$ -AR binding was conducted using rat cortical membranes. The binding assays contained 0.3 nM or 1.4 nM [<sup>3</sup>H]CGP-12177 in a volume of 1.0 mL for binding to  $\beta_2$ - and  $\beta_1$ -ARs, respectively. Non-specific binding was determined using 10  $\mu\text{M}$  propranolol. To block the  $\beta_2$ -AR sites present in the cortical membrane preparation, 30 nM ICI 118-551 was added to the assay buffer.

Competition curves with standard and unknown compounds included at least six concentrations, in triplicate.  $IC_{50}$  values and Hill coefficients were calculated using Prism software.  $K_i$  values were calculated using the Chang-Prusoff transformation.<sup>17</sup>

### 4.2. $\beta_2$ -AR mediated stimulation of cAMP accumulation

The HEK cells expressing  $\beta_2$ -ARs were grown on 96-well plates in DMEM containing 10% FBS, 0.05% penicillin–streptomycin, and 400  $\mu\text{g}/\text{mL}$  G418. When the cells reached confluence, the medium was removed and each well was rinsed with 0.1 mL of Krebs-HEPES buffer (130 mM NaCl, 4.8 mM KCl, 1.2 mM  $\text{KH}_2\text{PO}_4$ , 1.3 mM  $\text{CaCl}_2$ , 1.2 mM  $\text{MgSO}_4$ , 25 mM HEPES, and 10 mM glucose, pH 7.3). The test compound was diluted in Krebs-HEPES buffer containing 0.1% ascorbic acid, 10  $\mu\text{M}$  pargyline, and 50  $\mu\text{M}$  3-isobutyl-1-methylxanthine (IBMX), and 0.1 mL of the solution was added to each well. In the agonist assay, the plates were preincubated for 10 min at room temperature (rt) with buffer alone; then test compound diluted in buffer was added to the wells. In the antagonist assay, the plates were preincubated (for 20 min at 37 °C) with test compound diluted in buffer; then buffer plus 30 nM formoterol was added. The plates were incubated for an additional 10 min with the test compound. After incubation, the medium was removed and 0.1 mL of 0.5 M formic acid added. After a minimum of 1 h, the supernatant was removed and lyophilized. cAMP was quantified using the protein kinase binding assay of Gilman.<sup>18</sup> The amount of protein per well was determined and used to calculate the amount of cAMP/mg/well.

### 4.3. Cardiomyocyte contractility

These experiments were carried out as previously described.<sup>3</sup> In brief, single ventricular myocytes were isolated from 2–4 month old rat hearts by a standard enzymatic technique. The isolated cells were resuspended in HEPES buffer solution [20 mM, pH 7.4] containing, NaCl (137 mM), KCl (5.4 mM), MgCl<sub>2</sub> (1.2 mM), NaH<sub>2</sub>PO<sub>4</sub> (1.0 mM), CaCl<sub>2</sub> (1.0 mM), and glucose (20 mM). All experiments were performed within 8 h of cell isolation.

The cells were placed on the stage of an inverted microscope (Zeiss model IM-35, Zeiss, Thornwood, NY), perfused with the HEPES- buffered solution at a flow rate of 1.8 mL/min, and electrically stimulated at 0.5 Hz at 23 °C. Cell length was monitored by an optical edge-tracking method using a photodiode array (Model 1024 SAQ, Reticon, Boston, MA) with a 3 ms time resolution. Cell contraction was measured by the percent shortening of cell length following electrical stimulation.

### 4.4. Comparative molecular field analysis (CoMFA)

SYBYL 8.0. (TRIPOS Inc., St. Louis, MO) was used for 3D QSAR modeling. The previously described CoMFA model<sup>3</sup> was used for pK<sub>i</sub> prediction for the set of newly designed derivatives. Briefly, molecular models of structures were prepared in HyperChem v. 6.03 (HyperCube Inc., Gainesville, FL) using ModelBuild procedure to ensure the same conformation of the common scaffold. The models were extracted to SYBYL and the Gasteiger–Huckel atomic charges were calculated. The models were aligned with molecules of original training set using the two asymmetric carbon atoms in the core of the fenoterol molecule (–C\*–CH<sub>2</sub>–NH–C\*–CH<sub>2</sub>–) as a common substructure. A PREDICT procedure implemented in CoMFA package was used to compute the estimated pK<sub>i</sub> values.

The revised CoMFA ( $n = 32$ ) model was developed using a training set that included the new structures and pK<sub>i</sub> values examined in this study, that is, the (*R,R*)- and (*R,S*) isomers of **52**, **53**, **54**. Two types of molecular fields (steric and electrostatic) were sampled on the grid (2 Å spacing) lattice surrounding each structure. Distance-dependent dielectric constant was used in electrostatic calculations and energetic cutoffs of 30 kcal/mol for both the steric and the electrostatic energies were set.

The application of the partial Least Square correlation procedure to the resultant database extracted four significant components and validation parameters for this solution (CoMFA ( $n = 32$ )), which are presented in Table 4. For the sake of comparison the validity parameters obtained for the original solution (CoMFA ( $n = 26$ ))<sup>3</sup> are also included in Table 4.

### 4.5. Chemistry

All reactions were carried out using commercial grade reagents and solvents. Ultraviolet spectra were recorded on a Cary 50 Concentration spectrophotometer. Optical rotations were done at 25 °C on a Rudolph Research Autopol IV. NMR Spectra were recorded on a Varian Mercury VMX 300-MHz spectrophotometer. In reporting the NMR multiplicities, we used the following abbreviations: s, singlet; d, doublet; t, triplet; q, quartet; p, pentet; m, multiplet; apt., apparent; and br, broad. Low resolution mass spectra (MS) were obtained on a Finnigan LCQ<sup>DUO</sup> LC MS/MS system equipped with an electrospray ionization (ESI) probe. High resolution mass spectra (HRMS) were obtained by the University of Minnesota Mass Spectrometry Service, also with an ESI probe. Analytical HPLC data were obtained using a Waters 2690 Separations Module with PDA detection. Method (a): Varian Sunfire 100 × 4.6 mm C18 column. Method (b): ThermoHypersil BDS 100 × 4.6 mm C18 column. Method (c): Chiralpak IA 250 × 10 mm. Merck silica gel (230–400 mesh) was used for open column chromatography.

### 4.6. Synthesis of (*R,R*)- and (*R,S*)-fenoterol analogues

The fenoterol analogues used in this study were prepared following a previously reported synthetic scheme in which (*R*)-(–)-3',5'-dibenzoyloxyphenylbromohydrin or (*S*)-(+)-3',5'-dibenzoyloxyphenylbromohydrin was condensed with the appropriate free *N*-benzylaminoalkane.<sup>3</sup> The present work only utilized (*R*)-(–)-3',5'-dibenzoyloxy-phenylbromohydrin, which was synthesized as previously reported.<sup>3</sup> The syntheses of the new *N*-benzylaminoalkanes and fenoterol analogues are reported below.

### 4.7. General procedure for the preparation of aryl ketones

The appropriate phenylacetic acid and alkyl anhydride were combined in pyridine and heated to reflux under argon for 6 h. Solvents were removed and the residue was partitioned between dichloromethane and 1 N NaOH. The organic fraction was washed with water, dried (Na<sub>2</sub>SO<sub>4</sub>), filtered, and evaporated. Silica gel chromatography (1:30) eluting with 1/1 dichloromethane/hexanes affords the pure aryl ketone.

#### 4.7.1. 1-(4-(Benzyloxy)phenyl)butan-2-one

Prepared from 7.5 g (31 mmol) of 4-benzyloxyphenylacetic acid (Aldrich) and 17.2 mL of propionic anhydride in 17 mL of pyridine. Yield 1.92 g (24%). <sup>1</sup>H NMR (CDCl<sub>3</sub>) δ 1.00 (t, 3H, *J* = 7.5 Hz), 2.44 (q, 2H, *J* = 7.5, Hz), 3.59 (s, 2H), 5.02 (s, 2H), 6.90 (d, 2H, *J* = 8.7 Hz), 7.09 (d, 2H, *J* = 8.7 Hz), 7.25–7.40 (m, 5H) ppm.

#### 4.7.2. 1-(Naphthalen-2-yl)propan-2-one

Prepared from 25.0 g (134 mmol) of 2-naphthylacetic acid (Aldrich) and 100 mL of acetic anhydride in 100 mL of pyridine. Yield 3.68 g (15%). <sup>1</sup>H NMR (CDCl<sub>3</sub>) δ 2.19 (s, 3H), 3.86 (s, 2H), 7.35 (dd, 1H, *J* = 2.1, 8.7 Hz), 7.45–7.50 (m, 2H), 7.68 (s, 1H), 7.79–7.85 (m, 3H), ppm.

#### 4.7.3. 1-(4-Methoxynaphthalene-1-yl)propan-2-one

Prepared from 5.04 g (23.3 mmol) of 4-methoxy-1-naphthylacetic acid (ACB Blocks Ltd.) and 30 mL of acetic anhydride in 30 mL of pyridine. Yield 1.54 g (31%). <sup>1</sup>H NMR (CDCl<sub>3</sub>) δ 2.09 (s, 1H), 4.01 (s, 3H), 4.02 (s, 2H), 6.78 (d, 1H, *J* = 7.8 Hz), 7.29 (d, 1H, *J* = 7.8), 7.47–7.56 (m, 2H), 7.78–7.82 (m, 1H), 8.30–8.33 (m, 1H) ppm.

### 4.8. General procedure for the preparation of *N*-benzylaminoalkanes

To the appropriate aryl ketone in dichloromethane ( $c = 0.5$  M), cooled to 0 °C was added glacial acetic acid (1 equiv), followed by benzylamine (1 equiv) and Na(OAc)<sub>3</sub>BH (1.4 equiv). The reaction mixture was warmed to RT and stirred under argon for 20 h. Cooled reaction mixture (ice bath) and added dropwise 10% NaOH (5 equiv), then extracted into dichloromethane, washed with brine, dried (Na<sub>2</sub>SO<sub>4</sub>), filtered, and evaporated. The resulting product was used without further purification.

#### 4.8.1. *rac-N*-Benzyl-1-(4-(benzyloxy)phenyl)butan-2-amine

Prepared from 1.88 g (7.4 mmol) of 1-(4-(benzyloxy)phenyl)butan-2-one, 0.81 mL (7.4 mmol) of benzylamine, 2.40 g (11.3 mmol) of Na(OAc)<sub>3</sub>BH and 0.5 mL of acetic acid. Yield 2.55 g (100%). <sup>1</sup>H NMR (CDCl<sub>3</sub>) δ 0.93 (t, 3H, *J* = 7.2 Hz), 1.45–1.55 (m, 2H), 2.60–2.75 (m, 2H, 1H), 3.76 (dd, 2H, *J* = 6.6, 9.9 Hz), 5.03 (s, 2H), 6.88 (d, 2H, *J* = 8.7 Hz), 7.06 (d, 2H, *J* = 8.7 Hz), 7.18–7.45 (m, 10H) ppm. MS (ESI+) *m/z* (rel): 346 (100, M+H).

#### 4.8.2. *rac-N*-Benzyl-1-(naphthalen-2-yl)propan-2-amine

Prepared from 3.68 g (20 mmol) of 1-(naphthalen-2-yl)propan-2-one, 2.18 mL (20 mmol) of benzylamine, 6.35 g (30 mmol) of

Na(OAc)<sub>3</sub>BH and 1.3 mL of acetic acid. Yield 5.04 g (92%). <sup>1</sup>H NMR (CDCl<sub>3</sub>) δ 1.07 (d, 3H, *J* = 6.0 Hz), 2.70–2.91 (m, 2H), 2.97 (sextet, 1H, *J* = 6.6 Hz), 3.39 (s, 1H, NH), 3.75 (dd, 2H, *J* = 13.2, 34.2 Hz), 7.10–7.24 (m, 5H, 1H), 7.34–7.39 (m, 2H), 5.30 (s, 1H), 7.67–7.77 (m, 3H) ppm. MS (ESI+) *m/z* (rel): 276 (100, M+H).

#### 4.8.3. *rac-N-Benzyl-1-(4-methoxynaphthalen-1-yl)propane-2-amine*

Prepared from 1.48 g (6.9 mmol) of 1-(4-methoxynaphthalene-1-yl)propan-2-one, 0.75 mL (6.9 mmol) of benzylamine, 2.20 g (10.4 mmol) of Na(OAc)<sub>3</sub>BH and 0.45 mL of HOAc. Yield 1.96 g (93%). <sup>1</sup>H NMR (CDCl<sub>3</sub>) δ 1.15 (d, 3H, *J* = 6.0 Hz), 2.98–3.15 (m, 2H), 3.20–3.24 (m, 1H), 3.82 (dd, 3H, *J* = 13.8, 47.7 Hz), 3.99 (s, 3H), 6.73 (d, 1H, *J* = 7.8 Hz), 7.17–7.26 (m, 5H, 1H), 7.45–7.48 (m, 2H), 7.88–7.91 (m, 1H), 8.28–8.32 (m, 1H) ppm. MS (ESI+) *m/z* (rel): 306 (100, M+H).

#### 4.9. General procedure for the enantiomeric resolution of *N*-benzylaminoalkanes

The appropriate racemic *N*-benzylaminoalkane was combined with 1 equiv of either optically active mandelic acid or naproxen in 1:2 *i*PrOH/MeOH (*c* 0.5 M), refluxed until full dissolution, then cooled to rt. The crystals were filtered, collected, and recrystallized twice from MeOH (*c* 0.3 M) to afford the optically active salts. The salts were converted to the free amine by partitioning between 10% K<sub>2</sub>CO<sub>3</sub> and CHCl<sub>3</sub>, drying organic extracts (Na<sub>2</sub>SO<sub>4</sub>), filtering and evaporating.

#### 4.9.1. (*R*)-(–)-*N-Benzyl-1-(4-(benzyloxy)phenyl)butan-2-amine*

Prepared from 2.56 g (7.4 mmol) of *rac-N*-benzyl-1-(4-(benzyloxy)phenyl)butan-2-amine and 1.12 g (7.4 mmol) of (*R*)-(–)-mandelic acid (Aldrich). Yield 433 mg (33%), [ $\alpha$ ]<sub>D</sub> = –18.0 (0.7% MeOH).

#### 4.9.2. (*S*)-(+)-*N-Benzyl-1-(4-(benzyloxy)phenyl)butan-2-amine*

Prepared from 2.11 g (6.1 mmol) of *rac-N*-benzyl-1-(4-(benzyloxy)phenyl)butan-2-amine and 928 mg (6.1 mmol) of (*S*)-(+)-mandelic acid (Aldrich). Yield 407 mg (39%), [ $\alpha$ ]<sub>D</sub> = +21.4 (0.8% MeOH).

#### 4.9.3. (*R*)-(–)-*N-Benzyl-1-(naphthylen-2-yl)propan-2-amine*

Prepared from 1.05 g (3.8 mmol) of *rac-N*-benzyl-1-(naphthylen-2-yl)propan-2-amine and 875 mg (3.8 mmol) of (*S*)-(+)-naproxen (Aldrich). Yield 310 mg (61%), [ $\alpha$ ]<sub>D</sub> = –11.2 (0.7% MeOH).

#### 4.9.4. (*S*)-(+)-*N-Benzyl-1-(naphthylen-2-yl)propan-2-amine*

Prepared from 2.10 g (7.6 mmol) of *rac-N*-benzyl-1-(naphthylen-2-yl)propan-2-amine and 1.76 g (7.6 mmol) of (*R*)-(–)-naproxen (Aldrich). Yield 630 mg (60%), [ $\alpha$ ]<sub>D</sub> = +12.0 (0.7% MeOH).

#### 4.9.5. (*R*)-(–)-*N-Benzyl-1-(4-methoxynaphthalen-1-yl)propane-2-amine*

Prepared from 1.04 g (3.4 mmol) of *rac-N*-benzyl-1-(4-methoxynaphthalen-1-yl)propane-2-amine and 520 mg (3.4 mmol) of (*S*)-(+)-mandelic acid. Yield 389 mg (77%), [ $\alpha$ ]<sub>D</sub> = –12.1 (1.0% MeOH).

#### 4.9.6. (*S*)-(+)-*N-Benzyl-1-(4-methoxynaphthalen-1-yl)propane-2-amine*

Prepared from 1.95 g (6.4 mmol) of *rac-N*-benzyl-1-(4-methoxynaphthalen-1-yl)propane-2-amine and 971 mg (6.4 mmol) of (*R*)-(–)-mandelic acid. Yield 988 mg (67%), [ $\alpha$ ]<sub>D</sub> = +11.7 (1.0% MeOH).

#### 4.10. Preparation of fenoterol analogs

In this study, the fenoterol analogues were prepared using a previously described approach.<sup>3</sup> The key step involved the

coupling of the epoxide formed from (*R*)-(–)-3',5'-dibenzyloxyphenylbromohydrin with the (*R*)- or (*S*)-enantiomer of the appropriate *N*-benzylaminoalkanes. The epoxide was formed by combining (*R*)-(–)-3',5'-dibenzyloxyphenylbromohydrin (1 equiv) with K<sub>2</sub>CO<sub>3</sub> (1.4 equiv) in 1:1 THF/MeOH (*c* 0.3 M) and stirring for 2 h under argon at rt. The solvent was removed and the residue partitioned between toluene and H<sub>2</sub>O, the toluene fraction dried (Na<sub>2</sub>SO<sub>4</sub>), filtered, and evaporated. The residue was dissolved with 0.95 equiv of the appropriate free *N*-benzylaminoalkane in toluene and evaporated again under high vacuum to remove trace H<sub>2</sub>O. The resulting colorless residue was heated to 120 °C under argon for 24–48 h, monitoring by <sup>1</sup>H NMR and mass spectrometry to afford the coupled product. The residue was dissolved in EtOH (*c* 0.07 M) with heat and transferred to a Parr flask, where it was hydrogenated at 50 psi of hydrogen over 10% (wt) Pd/C (10 mg cat/65 mg bromohydrin) for 24 h to afford the debenzylated product, as confirmed by <sup>1</sup>H NMR and mass spectrometry. The mixture was filtered through Celite<sup>®</sup>, the filter cake rinsed with *i*PrOH, and then concentrated. The free base was purified on silica gel (1:20) eluting with 15% methanol/chloroform. The resulting material was converted to the fumarate salt by heating with 0.5 eq of fumaric acid in 1:1 *i*PrOH/EtOH (*c* 0.2 M) to afford the 0.5 fumarate salt of the fenoterol analog.

#### 4.10.1. (*R,R*)-(–)-5-(1-Hydroxy-2-(1-hydroxyphenyl)butan-2-ylamino)ethyl benzene-1,3-diol [(*R,R*)-52]

Prepared from 282 mg (0.82 mmol) of (*R*)-(–)-*N*-benzyl-1-(4-(benzyloxy)phenyl)butan-2-amine and 260 mg (0.78 mmol) of (*R*)-(–)-3',5'-dibenzyloxyphenylbromohydrin. Yield 175 mg (60%). <sup>1</sup>H NMR (300 MHz, CD<sub>3</sub>OD): δ 0.950 (t, 3H, *J* = 7.5 Hz), 1.67 (m, 2H), 2.83–3.18 (m, 4H), 3.33–3.40 (m, 1H), 3.37 (s, 4H), 4.82 (m, 1H), 6.24 (d, 1H, *J* = 2.1 Hz), 6.37 (d, 2H, *J* = 1.8 Hz), 6.73 (s, 2H, fum), 6.76 (d, 2H, *J* = 8.4 Hz), 7.05 (d, 2H, *J* = 8.7 Hz) ppm. <sup>13</sup>C NMR (75 MHz, CD<sub>3</sub>OD) δ 9.43, 23.28, 36.56, 52.29, 62.16, 70.02, 103.4, 105.3, 116.7, 127.8, 131.3, 136.5, 144.6, 157.6, 159.9, 172.3 ppm. UV (MeOH) λ<sub>max</sub> 206 nm ( $\epsilon$  22,500), 223 (12,300), 278 (2460); [ $\alpha$ ]<sub>D</sub> = –15.6 (free amine, 0.5% MeOH); HPLC: (a) H<sub>2</sub>O/ACN/TFA 70/30/0.01, 1.0 mL/min, 278 nm, *t*<sub>R</sub> = 3.57 min, 97.1% pure. (c) ACN/MeOH/TFA 90/10/0.05, 2.0 mL/min, 278 nm, *t*<sub>R</sub> = 5.26 min, 97.5% enantiomeric purity. HRMS (*m/z*) calcd for C<sub>18</sub>H<sub>24</sub>NO<sub>4</sub> [M+H]<sup>+</sup> 318.1700; found 318.1699.

#### 4.10.2. (*R,S*)-(+)-5-(1-Hydroxy-2-(1-hydroxyphenyl)butan-2-ylamino)ethyl benzene-1,3-diol [(*R,S*)-52]

Prepared from 352 mg (1.02 mmol) of (*S*)-(+)-*N*-benzyl-1-(4-(benzyloxy)phenyl)butan-2-amine and 321 mg (0.97 mmol) of (*R*)-(–)-3',5'-dibenzyloxyphenylbromohydrin. Yield 142 mg (38%). <sup>1</sup>H NMR (300 MHz, CD<sub>3</sub>OD): δ 0.972 (t, 3H, *J* = 7.5 Hz), 1.70 (p, 2H, *J* = 6.9 Hz), 2.86–3.22 (m, 4H), 3.32–3.37 (m, 1H), 3.34 (s, 4H), 4.82 (m, 1H), 6.25 (t, 1H, *J* = 2.1 Hz), 6.36 (d, 2H, *J* = 1.8 Hz), 6.74 (s, 2H, fum), 6.77 (d, 2H, *J* = 8.4 Hz), 7.08 (d, 2H, *J* = 8.7 Hz) ppm. <sup>13</sup>C NMR (75 MHz, CD<sub>3</sub>OD) δ 9.820, 24.16, 36.48, 52.30, 62.32, 69.92, 103.3, 105.3, 116.8, 127.7, 131.3, 136.1, 144.4, 157.6, 159.8, 171.3 ppm. UV (MeOH) λ<sub>max</sub> 204 nm ( $\epsilon$  26,900), 224 (11,500), 278 (2320). [ $\alpha$ ]<sub>D</sub> = –7.2 (free amine, 0.5% MeOH). HPLC: (a) H<sub>2</sub>O/ACN/TFA 70/30/0.01, 1.0 mL/min, 278 nm, *t*<sub>R</sub> = 3.56 min, 99.5% pure. (c) ACN/MeOH/TFA 90/10/0.05, 2.0 mL/min, 278 nm, *t*<sub>R</sub> = 5.88 min, 99.0% enantiomeric purity. HRMS (*m/z*): calcd for C<sub>18</sub>H<sub>24</sub>NO<sub>4</sub> [M+H]<sup>+</sup> 318.1700; found 318.1706.

#### 4.10.3. (*R,R*)-5-(1-Hydroxy-2-(1-(naphthalen-2-yl)propan-2-ylamino)ethyl) benzene-1,3-diol [(*R,R*)-53]

Prepared from 310 mg (1.12 mmol) of (*R*)-(–)-*N*-benzyl-1-(naphthylen-2-yl)propan-2-amine and 355 mg (1.06 mmol) of (*R*)-(–)-3',5'-dibenzyloxyphenylbromohydrin. Yield 186 mg (44%). <sup>1</sup>H NMR (300 MHz, CD<sub>3</sub>OD): δ 1.06 (d, 3H, *J* = 6.3 Hz), 2.73–2.90

(m, 4H), 3.07 (m, 1H), 3.30 (m, 3H), 4.05 (dd, 1H,  $J = 5.1, 8.4$  Hz), 6.11 (t, 1H,  $J = 2.4$  Hz), 6.28 (d, 2H,  $J = 2.1$  Hz), 7.26 (dd, 1H,  $J = 1.5, 8.4$  Hz), 7.38–7.42 (m, 2H), 7.57 (s, 1H), 7.72–7.77 (m, 3H) ppm.  $^{13}\text{C}$  NMR (75 MHz,  $\text{CD}_3\text{OD}$ )  $\delta$  15.84, 40.67, 52.70, 56.66, 70.46, 103.27, 105.26, 126.97, 127.39, 128.22, 128.64, 128.70, 129.20, 129.64, 134.04, 135.05, 135.11, 136.81, 144.95, 160.13, 173.20 ppm. UV (MeOH),  $\lambda_{\text{max}}$ : 276 nm ( $\epsilon$  6170), 224 (90,680), 206 (50,290);  $[\alpha]_{\text{D}} = -27.4$  (0.5% MeOH). HPLC: (b)  $\text{H}_2\text{O}/\text{ACN}/\text{TFA}$  70/30/0.1, 1.0 mL/min, 275 nm,  $t_{\text{R}} = 3.96$  min, 95.3% purity. (c)  $\text{ACN}/i\text{PrOH}/\text{DEA}$  95/5/0.05, 3.0 mL/min, 275 nm,  $t_{\text{R}} = 8.58$  min, 95.6% enantiomeric purity. HRMS ( $m/z$ ): calcd for  $\text{C}_{21}\text{H}_{24}\text{NO}_3$   $[\text{M}+\text{H}]^+$  338.1751; found 338.1745.

#### 4.10.4. (R,S)- 5-(1-Hydroxy-2-(1-(naphthalen-2-yl)propan-2-ylamino)ethyl) benzene-1,3-diol [(R,S)-53]

Prepared from 626 mg (2.27 mmol) of (S)-(+)-N-benzyl-1-(naphthalen-2-yl)propan-2-amine and 719 mg (2.16 mmol) of (R)-(-)-3',5'-dibenzyloxyphenylbromohydrin. Yield 578 mg (68%).  $^1\text{H}$  NMR (300 MHz,  $\text{CD}_3\text{OD}$ ):  $\delta$  1.09 (d, 3H,  $J = 6.3$  Hz), 2.60–2.95 (m, 4H), 3.03 (m, 1H), 3.30 (m, 3H), 4.07 (dd, 1H,  $J = 5.1, 8.4$  Hz), 6.14 (t, 1H,  $J = 2.4$  Hz), 6.28 (d, 2H,  $J = 2.1$  Hz), 7.33 (dd, 1H,  $J = 1.8, 8.4$  Hz), 7.40–7.44 (m, 2H), 7.64 (s, 1H), 7.77–7.81 (m, 3H) ppm.  $^{13}\text{C}$  MNR (75 MHz,  $\text{CD}_3\text{OD}$ )  $\delta$  16.52, 40.28, 52.82, 56.88, 70.75, 103.27, 105.29, 126.97, 127.39, 128.22, 128.64, 128.69, 129.20, 129.65, 134.03, 135.05, 135.18, 136.89, 144.95, 160.00, 173.46 ppm. UV (MeOH),  $\lambda_{\text{max}}$ : 276 ( $\epsilon$  6310), 224 (93,530), 204 (50,580).  $[\alpha]_{\text{D}} = -18.8$  (0.5% MeOH). HPLC: (b)  $\text{H}_2\text{O}/\text{ACN}/\text{TFA}$  70/30/0.1, 1.0 mL/min, 275 nm,  $t_{\text{R}} = 3.94$  min, 98.6% purity. (c)  $\text{ACN}/i\text{PrOH}/\text{DEA}$  95/5/0.05, 3.0 mL/min, 275 nm,  $t_{\text{R}} = 8.04$  min, 96.4% enantiomeric purity. HRMS ( $m/z$ ): calcd for  $\text{C}_{21}\text{H}_{24}\text{NO}_3$   $[\text{M}+\text{H}]^+$  338.1751, found 338.1746.

#### 4.10.5. (R,R)-(-)-5-(1-Hydroxy-2-(1-(4-methoxynaphthalen-1-yl)propan-2-ylamino)ethyl)benzene-1,3-diol [(R,R)-54]

Prepared from 390 mg (1.28 mmol) of (R)-(-)-N-benzyl-1-(4-methoxynaphthalen-1-yl)propane-2-amine and 404 (1.22 mmol) of (R)-(-)-3',5'-dibenzyloxyphenylbromohydrin. Yield 309 mg (60%).  $^1\text{H}$  NMR (300 MHz,  $\text{CD}_3\text{OD}$ ):  $\delta$  1.22 (t, 3H,  $J = 6.6$  Hz), 3.09–3.21 (m, 3H), 3.59–3.69 (m, 2H), 3.99 (s, 3H), 4.74–4.83 (m, 1H), 6.23 (t, 1H,  $J = 2.4$  Hz), 6.37 (dd, 2H,  $J = 2.4, 5.7$  Hz), 6.74 (s, 1H), 6.86 (d, 1H,  $J = 7.8$  Hz), 7.32 (d, 1H,  $J = 7.8$  Hz), 7.48 (t, 1H,  $J = 6.9$  Hz), 7.56 (t, 1H,  $J = 6.9$  Hz), 8.02 (dd, 1H,  $J = 8.4, 12.0$  Hz), 8.27 (d, 1H,  $J = 8.7$  Hz) ppm.  $^{13}\text{C}$  NMR (75 MHz,  $\text{CD}_3\text{OD}$ ):  $\delta$  15.78, 36.66, 52.39, 55.96, 70.20, 103.4, 104.5, 105.3, 123.8, 124.3, 124.9, 126.2, 127.4, 128.1, 129.5, 133.8, 135.2, 144.6, 156.6, 160.0, 168.3 ppm. UV (MeOH),  $\lambda_{\text{max}}$ : 298 nm ( $\epsilon$  4,970), 286 (9920), 234 (22,600), 210 (42,500).  $[\alpha]_{\text{D}} = -28.8$  (free amine; 0.5% MeOH). HPLC: (a)  $\text{H}_2\text{O}/\text{ACN}/\text{TFA}$  50/50/0.01, 1.0 mL/min, 286 nm,  $t_{\text{R}} = 3.087$  min, 99.0% pure. (c) Gradient 0–20%  $i\text{PrOH}/\text{hexane}/0.05\%$  TFA, 3.0 mL/min, 275 nm,  $t_{\text{R}} = 8.62$  min, 95.0% enantiomeric purity. HRMS ( $m/z$ ): calcd for  $\text{C}_{22}\text{H}_{26}\text{NO}_4$   $[\text{M}+\text{H}]^+$  368.1856; found 368.1845.

#### 4.10.6. (R,S)-(+)-5-(1-Hydroxy-2-(1-(4-methoxynaphthalen-1-yl)propan-2-ylamino)ethyl)benzene-1,3-diol [(R,S)-54]

Prepared from 422 mg (1.38 mmol) of (S)-(+)-N-benzyl-1-(4-methoxynaphthalen-1-yl)propane-2-amine and 438 (1.31 mmol) of (R)-(-)-3',5'-dibenzyloxyphenylbromohydrin. Yield 302 mg

(53%).  $^1\text{H}$  NMR (300 MHz,  $\text{CD}_3\text{OD}$ ):  $\delta$  1.20 (t, 3H,  $J = 6.6$  Hz), 3.07–3.21 (m, 3H), 3.52–3.75 (m, 2H), 3.97 (s, 3H), 4.69–4.83 (m, 1H), 6.24 (t, 1H,  $J = 2.1$  Hz), 6.39 (dd, 2H,  $J = 2.4, 5.4$  Hz), 6.74 (s, 1H), 6.84 (d, 1H,  $J = 7.8$  Hz), 7.31 (d, 1H,  $J = 8.1$  Hz), 7.48 (t, 1H,  $J = 6.9$  Hz), 7.56 (t, 1H,  $J = 6.9$  Hz), 8.01 (dd, 1H,  $J = 8.4, 13.5$  Hz), 8.27 (d, 1H,  $J = 7.8$  Hz) ppm.  $^{13}\text{C}$  NMR (75 MHz,  $\text{CD}_3\text{OD}$ )  $\delta$  15.77, 36.64, 52.37, 55.94, 70.46, 103.4, 104.5, 105.3, 123.8, 124.3, 124.9, 126.2, 127.4, 128.1, 129.4, 133.8, 135.5, 144.7, 156.6, 160.0, 169.0 ppm. UV (MeOH),  $\lambda_{\text{max}}$ : 298 nm ( $\epsilon$  5430), 286 (5710), 233 (25,100), 210 (43,200).  $[\alpha]_{\text{D}} = -15.8$  (free amine; 0.5% MeOH). HPLC: (a)  $\text{H}_2\text{O}/\text{ACN}/\text{TFA}$  50/50/0.01, 1.0 mL/min, 286 nm,  $t_{\text{R}} = 3.087$  min, 96.0% pure (c) gradient 0–20%  $i\text{PrOH}/\text{hexane}/0.05\%$  TFA, 3.0 mL/min, 275 nm,  $t_{\text{R}} = 9.69$  min 99.0% enantiomeric purity. HRMS ( $m/z$ ): calcd for  $\text{C}_{22}\text{H}_{26}\text{NO}_4$   $[\text{M}+\text{H}]^+$  368.1856; found 368.1844.

#### Acknowledgments

This work was supported in part by funds from the National Institute on Aging, Intramural Research Program, NIA Contract N01-AG-3-1009 and the Foundation for Polish Science (FOCUS 4/2006 programme)

#### Supplementary data

Supplementary data associated with this article can be found, in the online version, at doi:10.1016/j.bmc.2009.11.062.

#### References and notes

- Xiao, R.-P.; Zhu, W.; Zheng, M.; Chakir, K.; Bond, R.; Lakatta, E. G.; Cheng, H. *Trends Pharmacol. Sci.* **2004**, *25*, 358–365.
- Beigi, F.; Bertucci, C.; Zhu, W.; Chakir, K.; Wainer, I. W.; Xiao, R.-P.; Abernethy, D. A. *Chirality* **2006**, *18*, 822–827.
- Jozwiak, K.; Khalid, C.; Tanga, M. J.; Berzetei-Gurske, I.; Jimenez, L.; Kozocas, J. A.; Woo, A.; Zhu, W.; Xiao, R.-P.; Abernethy, D. R.; Wainer, I. W. *J. Med. Chem.* **2007**, *50*, 2903–2915.
- Kikkawa, H.; Isogaya, M.; Nagao, T.; Kurose, H. *Mol. Pharmacol.* **1998**, *53*, 128–134.
- Isogaya, M.; Yamagiwa, Y.; Fujita, S.; Sugimoto, Y.; Nago, T.; Kurose, H. *Mol. Pharmacol.* **1998**, *54*, 616–622.
- Furse, K. E.; Lybrand, T. P. *J. Med. Chem.* **2003**, *46*, 4450–4462.
- Kubinyi, H. *Comparative Molecular Field Analysis (COMFA)*. In *Encyclopedia of Computational Chemistry*, 1998, John Wiley & Sons, Ltd. <http://www.wiley.com/legacy/wileychi/eec/>.
- Seifert, R.; Dove, S. *Mol. Pharmacol.* **2009**, *75*, 13–18.
- Cherezov, V.; Rosenbaum, D. M.; Hanson, M. A.; Rasmussen, S. G.; Thian, F. S.; Kobilka, T. S.; Choi, H. J.; Kuhn, P.; Weis, W. I.; Kobilka, B. K.; Stevens, R. C. *Science* **2007**, *318*, 1258–1265.
- Woo, A. Y.-H.; Wang, T.-B.; Zeng, X.; Weizog, Z.; Abernethy, D. R.; Wainer, I. W.; Xiao, R.-P. *Mol. Pharmacol.* **2009**, *75*, 158–165.
- Wieland, K.; Zuurmond, H. M.; Krasel, C.; Ijzerman, A. D. P.; Lohse, M. *J. Proc. Natl. Acad. Sci. U.S.A.* **1996**, *93*, 9276–9281.
- Zuurmond, H. M.; Hessling, J.; Blüml, K.; Lohse, M.; Ijzerman, A. P. *Mol. Pharmacol.* **1999**, *56*, 909–916.
- Kontoyianni, M.; DeWeese, C.; Penzotti, J. E.; Lybrand, T. P. *J. Med. Chem.* **1996**, *39*, 4406–4420.
- Swaminath, G.; Xiang, Y.; Lee, T. W.; Steenhuis, J.; Parnot, C.; Kobilka, B. K. *J. Biol. Chem.* **2004**, *279*, 686–691.
- Kobilka, B. *Mol. Pharmacol.* **2004**, *65*, 1060–1062.
- Staehelin, M.; Simons, P.; Jaeggi, K.; Wigger, N. *J. Biol. Chem.* **1983**, *258*, 3496–3502.
- Cheng, Y.-C.; Prusoff, W. H. *Biochem. Pharmacol.* **1973**, *22*, 3099–3108.
- Gilman, A. G. *Proc. Natl. Acad. Sci. U.S.A.* **1970**, *67*, 305–312.